

ChemComm

Accepted Manuscript



This is an *Accepted Manuscript*, which has been through the Royal Society of Chemistry peer review process and has been accepted for publication.

Accepted Manuscripts are published online shortly after acceptance, before technical editing, formatting and proof reading. Using this free service, authors can make their results available to the community, in citable form, before we publish the edited article. We will replace this *Accepted Manuscript* with the edited and formatted *Advance Article* as soon as it is available.

You can find more information about *Accepted Manuscripts* in the [Information for Authors](#).

Please note that technical editing may introduce minor changes to the text and/or graphics, which may alter content. The journal's standard [Terms & Conditions](#) and the [Ethical guidelines](#) still apply. In no event shall the Royal Society of Chemistry be held responsible for any errors or omissions in this *Accepted Manuscript* or any consequences arising from the use of any information it contains.

COMMUNICATION

Crystallographic determinations of solid-state structural transformations in a dynamic metal-organic framework

Cite this: DOI: 10.1039/x0xx00000x

Received 00th January 2012,
Accepted 00th January 2012Gui-Lian Li,^a Guang-Zhen Liu,^{*a} Lu-Fang Ma,^a Ling-Yun Xin,^a Xiao-Ling Li^a and Li-Ya Wang^{*,a,b}

DOI: 10.1039/x0xx00000x

www.rsc.org/

Various solid-state transformations in a metal-organic framework were determined by X-ray crystallography.

Metal-organic frameworks (MOFs) with structurally dynamic properties have attracted extreme interest due to their unique potential in switching, sensing, transport, and storage etc.^{1,2} Implementation of MOFs with single-crystal to single-crystal (SC-SC) structural transformation would enable clear expression of such dynamic features,³ because the single crystal X-ray crystallography paves the way for the accurate determination of the intermediates during the solid-state transformations that are typically involved in a significant rearrangement of structure motifs in the crystals including rotation, bending, swinging, sliding, or even cleavage/formation of chemical bonds.⁴ Unfortunately, there are not many dynamic MOFs with the ability to undergo a SC-SC transformation, as such crystals usually do not survive large degree of structure deformations.⁵ Generally, the solid-state transformation mechanisms were indirectly investigated through vibrational spectroscopy to monitor the topotactic nature, solid-state NMR to probe the conformational details of possible intermediates, and atomic force microscopy AFM techniques to explore the surface properties etc.⁶

Herein, we presented a new 3D “soft” MOF, [Zn₃(nbdc)₂(bpe)₂(OH)₂·H₂O·C₂H₅OH (1·H₂O·C₂H₅OH) (H₂nbdc = 4-nitrobenzene-1,2-bicarboxylic acid and bpe = 1,2-di(4-pyridyl)ethylene), prepared by hydrothermal reaction of Zn(OAc)₂·2H₂O, H₂nbdc, and bpe in EtOH-H₂O. The phase purity of the bulk material was confirmed by powder X-ray diffraction (PXRD) (Fig. S1, ESI†). Single crystal X-ray diffraction (SCXRD) revealed that 1·H₂O·C₂H₅OH consists of a linear trinuclear [Zn₃N₄(μ₂-OH)₂(COO)₄], dictating the overall framework topology of (6².8) *cds*. The framework consists of two types of cage structures identified as A and B, of which two smaller cages A at the channel corners accommodated by one H₂O molecule and two nbdc linkers, and the larger cage B at the channel centre filled with one EtOH molecule possesses a sphere-like shape surrounded by four nbdc linkers. Each unit cell contains four cages (2A and 2B) with each cage A accommodated by one H₂O molecule and each cage B filled with one EtOH molecule (Fig. S2-S6, ESI†). The hierarchical pore structures provide a desired platform allowing for detailed exploration of the SC-SC structural transformations

including reversible desolvation-resolvation, I₂ uptake-release, and photochemical [2+2] cycloaddition.

Thermogravimetric analysis (TGA) (Fig. S7, ESI†) and variable-temperature powder X-ray diffractions (VTPXRD) (Fig. S8, ESI†) showed that the air-stable crystals of 1·H₂O·C₂H₅OH can maintain good crystallinity and framework integrity at least before 240°C. It is noted that 1·H₂O·C₂H₅OH can suffer from various SC-SC desolvated-resolvated structural transformations (Fig. 1). Wherein the solvent-free phase 1 is hard to be captured because a rapid and dynamic rehydration process (Fig. S9 and S10, ESI†) is completed within several minutes in air to give a hydrated phase 1·H₂O·2.5H₂O (Table S1, ESI†) with one H₂O molecule located in cage A and 2.5H₂O molecules accommodated in cage B.

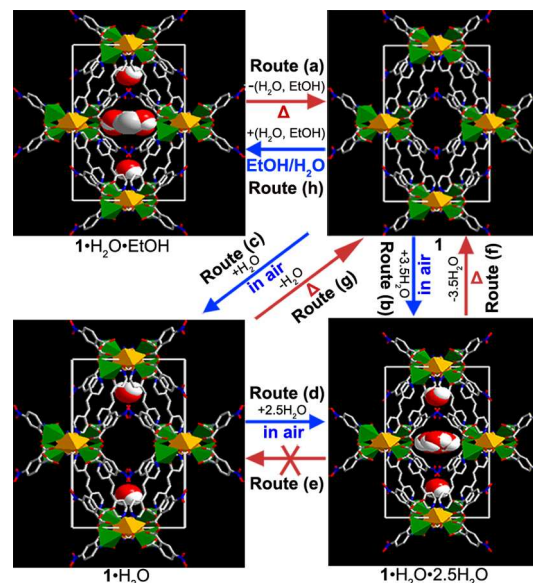


Fig. 1. Schematic representation of various SC-SC desolvated-resolvated behaviors for 1·H₂O·C₂H₅OH with different routes labeled as **Route a**→**h**.

Fortunately, we succeeded in capturing an intermediate during the hydration of 1 to give a partly hydrated phase 1·H₂O (Table S1, ESI†)

with one H₂O molecule accommodated in cage A leaving cage B still empty. This clearly shows that the water molecules firstly fill the smaller cage A, then occupy the larger cage B, that is, 1·H₂O is the intermediate from 1 to 1·H₂O·2.5H₂O. It is reasonable to propose that water molecule can diffuse into the cage A from the cage B through the side window between them, considering that the cage A has no pore opening in the crystal surface to allow for the direct access of guest molecule. The filling of the smaller then the larger adsorption sites is consistent with the theory of micropore filling,⁷ indicating a two-step pore-filling sequence.⁸ Such fast water adsorption behavior in air in a SC-SC manner is a rarely observed phenomenon in coordination polymers.⁹

Furthermore, the exposure of crystal 1 to mixed EtOH/H₂O vapours makes it restore to 1·H₂O·C₂H₅OH in a SC-SC manner, implying a stronger EtOH affinity over H₂O for the cage B; this prompts us to examine iodine-uploaded capacity of the microporous framework. The crystals appear a remarkable change of color from colorless to violet after suspending 1·H₂O·C₂H₅OH in iodine cyclohexane solution for a period of time. Thiosulfate determination of the iodine content by the release of I₂ into ethanol solution gave 1.07I₂ for three zinc atoms. The photographs (Fig. S11, ESI†) showed that the “static” iodine release without disturbing the crystals induces the color of solution gradually appearing violet with increasing time, and the “kinetic” iodine release with constant stirring explored by time-dependent UV/vis spectroscopy displays the absorption maximum λ_{\max} at 206, 226, 288 and 360 nm becoming stronger with increasing iodine content in the ethanol (Fig. S12, ESI†). The intensity of absorption band at 206 nm is proportional to concentration of I₂ molecule, and the absorption bands at 288 and 360 nm correspond to polyiodide I₃⁻ anion that is generally stabilized by H⁺ ion. It is shown that the delivery of iodine increases linearly with increasing time at least in first 90 min, whereas a complete iodine release needs more than two weeks to reach the equilibrium state, implying that the iodine delivery is governed by a strong host-guest interaction, in contrast to conventional iodine adsorbent materials lacking an accessible well-defined host-guest interaction.¹⁰

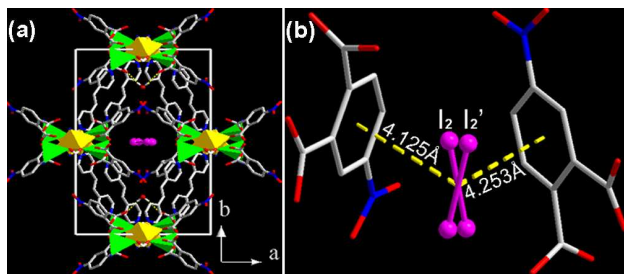


Fig. 2. (a) The cell unit of 1·H₂O·I₂. (b) The relative position between the disordered I₂ molecule and nbdc ligands.

The SCXRD (Table S1, ESI†) showed that the EtOH guest in cage B was exchanged by one I₂ molecule disordered over two positions, leaving the H₂O guest in cage A static (Fig. 2). The TGA (Fig. S13, ESI†) showed that a value of $x \approx 0.94$ was obtained by taking into account one water guest for per molecular formula 1·H₂O·xI₂, which is consistent with thiosulfate determination and SCXRD analysis. The I₂ affinity of 1·H₂O·C₂H₅OH may be attributed to regular π -electron-rich wall of the cage B made of four nbdc carboxylate ligands. The separation between the centre of I-I bond and the centroid of the benzene ring of nbdc ligand ranges from 4.125 to 4.253 Å, probably forming CT-complex between I₂ and benzene rings (CT = charge transfer),¹¹ which achieves a better controlled uptake and release of I₂. The calculated density of 1·H₂O·I₂ (1.907 g/cm³) increased remarkably (ca. 19.8%) relative to that of 1·H₂O·C₂H₅OH (1.591 g/cm³). A few examples of iodine

inclusion into organic/inorganic porous frameworks¹² and into MOFs^{10,13} have been known, however, the reports on iodine adsorption of MOFs in a SC-SC manner only recently emerged, to the best of our knowledge.¹⁴ Probably, the inclusion of I₂ requires to break original host-guest H-bonding interactions and to reconstruct new host-guest interactions such as CT-complex and halogen bonds, which creates strain to make the crystal present a certain degree of pulverization.

Furthermore, the distance between the centres of the C=C bonds of parallel positioned bpe ligands is 3.738 Å (less than 4.2 Å), satisfying the topophotocatalytic criteria established by Schmidt.¹⁵ It is noted that there are two different orientated bpe pairs bridging the trimeric Zn₃ units to form two uniform ladder motifs propagating along the [110] and [1-10] direction, respectively. Such structural features provide an ideal model to study the details of the solid-state photodimerization of C=C bonds. Upon UV irradiation of 1·H₂O·C₂H₅OH for a period of time, the crystals display a color change from colorless to yellow. The X-ray crystallography showed that 1·H₂O·C₂H₅OH can also convert to 1·H₂O·2.5H₂O resulting from the evacuation of EtOH guest when UV irradiation above 6h and the subsequent rehydration after removing the light. The ¹H NMR spectra showed the signals from olefinic protons ($\delta = 7.54$ ppm) gradually weaken, accompanying with the appearance of the signals of the cyclobutane protons ($\delta = 4.67$ ppm) as prolonged irradiated time, and the shifted signals of bipyridine protons gradually strengthen ($\delta = 8.35$ and 7.24 ppm), coupling with the gradually weakened signals from unreacted bpe ligands ($\delta = 8.60$ and 7.62 ppm) (Fig. S14, ESI†). The observed chemical shifts implied that parallel positioned bpe ligands are partly transformed into stereo-specific *rcctt*-tpcb regioisomer (Fig. S15, ESI†)¹⁶ and that the prolonged irradiation can improve the percentage of photodimerized product; finally reaching a maximum 78% [2+2] cycloaddition after irradiation for 63h. Due to the loss of the single crystalline nature, the solid-state structure of the final photochemical product could not be determined by SCXRD.

Fortunately, a 50% photoreactive intermediate, [Zn₃(nbdc)₂(*rcctt*-tpcb)_{0.5}(bpe)_{0.5}(OH)₂·H₂O·0.5H₂O (2) (Table S1, ESI†), was successfully captured by irradiating crystals of 1·H₂O·C₂H₅OH for 13h (Fig. 3). The SCXRD showed that the framework almost remains unchanged (Fig. S16, ESI†) except for the local formation of new C-C bonds across the ethylene bonds between parallel bpe ligands along the [1-10] direction, whereas parallel bpe ligands along the [110] direction only display a degree of the distortion. For unreacted bpe pairs, the C...C distance of 1.508 Å within bpe ligands is larger than 1.319 Å of initial C=C bond and comparable to that of normal C-C bond, but the C...C distance of 2.226 Å between parallel bpe ligands is much less than the separation of 3.738 Å across two initial C=C bonds. It is clear that 1·H₂O·C₂H₅OH displays an extremely anisotropic photoreactivity along the [110] and [1-10] directions. In the formation of the cyclobutane derivative, the cleavage and formation of chemical bonds is gradual rather than sharp, probably undergoing a series of transition states. To the best of our knowledge, both the anisotropic photoreactivity and the gradual transformation mechanism are firstly observed in MOFs.

To date, there is only two reports on the photochemical [2+2] cycloaddition of 3D MOFs,¹⁷ in addition to a pillared-layer, [Mn₂(HCO₃)₃(bpe)₂(H₂O)₂]ClO₄·H₂O·bpe¹⁸ with a 60% photoreactivity between bridging bpe ligands and lattice bpe molecules, wherein the hydrogen-bonded bpe in the lattice probably provided the flexibility needed for photoreactivity. Usually, the bridging ligands are interlocked at both terminals such that the movements are restricted upon metal coordination. In such 3D cases, although the ligands have been found in parallel arrangements, the solids may not be photoreactive¹⁹ despite satisfying Schmidt's

criteria. Most of the dimerization reactions usually occur in various organic compounds, metal complexes as well as low-dimensional coordination polymers (1D and 2D).^{16,20} The photoreactivity of $1 \cdot \text{H}_2\text{O} \cdot \text{C}_2\text{H}_5\text{OH}$ implies that its framework can suffer from a relatively high degree of structure deformation.

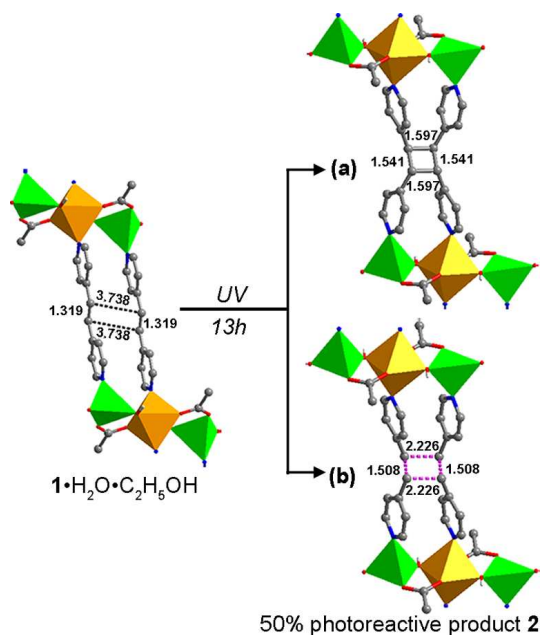


Fig. 3. Schematic evolution of photodimerized reaction for $1 \cdot \text{H}_2\text{O} \cdot \text{C}_2\text{H}_5\text{OH}$. (a) and (b) representing two kinds of local geometry configurations for reacted and unreacted bpe ligands in the 50% photoreactive product 2.

In summary, “soft” MOFs can suffer from various solid-state structural transformations with the framework retaining high integrity. The crystalline solids with hierarchical pore structures are inclined to a stepwise pore-filling during guest uptake, whereas the transport of I_2 is facilitated by unique host-guest interactions such as CT-complex. Solid-state photochemical [2+2] cycloaddition is extremely anisotropic and related to gradual rather than sharp cleavage and formation of chemical bonds.

This work was supported by the National Natural Science Foundation of China (No. 20971064 and No. 21271098) and by the Foundation for University Young Key Teacher by Henan Province of China (Grant No. 2011GGJS-153).

Notes and references

^a College of Chemistry and Chemical Engineering, Luoyang Normal University, Luoyang, Henan 471022, China. E-mail: gzliuyl@126.com.

^b College of Chemistry and Pharmacy Engineering, Nanyang Normal University, Nanyang, Henan 473061, China. E-mail: wlya@lynu.edu.cn.

† Electronic Supplementary Information (ESI) available: Experimental and synthetic details, Table S1-S3 and Fig. S1-S16. CCDC 972455-972459. For ESI and crystallographic data in CIF or other electronic format. See DOI: 10.1039/c000000x/

- (a) G. J. Halder, C. J. Kepert, B. Moubaraki, K. S. Murray and J. D. Cashion, *Science*, 2002, **298**, 1762; (b) S. Kitagawa, R. Kitaura and S.-i. Noro, *Angew. Chem. Int. Ed.*, 2004, **43**, 2334. (c) C. J. Kepert, *Chem. Commun.*, 2006, 695.
- (a) Y.-M. Song, F. Luo, M.-B. Luo, Z.-W. Liao, G.-M. Sun, X.-Z. Tian, Y. Zhu, Z.-J. Yuan, S.-J. Liu, W.-Y. Xu and X.-F. Feng, *Chem.*

- Commun.*, 2012, **48**, 1006; (b) C. Avendano, Z. Zhang, A. Ota, H. Zhao and K. R. Dunbar, *Angew. Chem. Int. Ed.*, 2011, **50**, 6543; (c) J. Liu, Y.-X. Tan and J. Zhang, *Cryst. Growth Des.*, 2012, **12**, 5164.
- (a) J. J. Vittal, *Coord. Chem. Rev.*, 2007, **251**, 1781; (b) M.-S. Chen, M. Chen, S. Takamizawa, T. Okamura, J. Fan and W.-Y. Sun, *Chem. Commun.*, 2011, **47**, 3787; (c) G.-C. Lv, P. Wang, Q. Liu, J. Fan, K. Chen and W.-Y. Sun, *Chem. Commun.*, 2012, **48**, 10249; (d) H.-X. Zhang, F. Wang, Y.-X. Tan, Y. Kang and J. Zhang, *J. Mater. Chem.*, 2012, **22**, 16288.
 - (a) S. Kitagawa and K. Uemura, *Chem. Soc. Rev.*, 2005, **34**, 109; (b) A. M. Chippindale and S. J. Hibble, *J. Am. Chem. Soc.*, 2009, **131**, 12736.
 - (a) T. Kawamichi, T. Haneda, M. Kawano and M. Fujita, *Nature*, 2009, **461**, 633; (b) D. X. Xue, W. X. Zhang, X. M. Chen and H. Z. Wang, *Chem. Commun.*, 2008, 1551.
 - Y. Ohashi, *Models, Mysteries and Magic of Molecules* (Eds.: J. C. A. Boeyens and J. F. Ogilvie), Springer, Berlin, 2008, pp. 109–113.
 - F. Rouquerol, J. Rouquerol and K. Sing, *Adsorption by Powders & Porous Solids*, Academic Press, San Diego, 1998.
 - (a) C. Yang, X. Wang and M. A. Omary, *J. Am. Chem. Soc.*, 2007, **129**, 15454; (b) C. Yang, X. P. Wang and M. A. Omary, *Angew. Chem. Int. Ed.*, 2009, **48**, 2500.
 - (a) X.-Y. Dong, B. Li, B.-B. Ma, S.-J. Li, M.-M. Dong, Y.-Y. Zhu, S.-Q. Zang, Y. Song, H.-W. Hou and T. C. W. Mak, *J. Am. Chem. Soc.*, 2013, **135**, 10214; (b) C.-L. Chen, A. M. Goforth, M. D. Smith, C.-Y. Su and H.-C. Loye, *Angew. Chem. Int. Ed.*, 2005, **44**, 6673.
 - M.-H. Zeng, Q.-X. Wang, Y.-X. Tan, S. Hu, X.-H. Zhao, L.-S. Long and M. Kurmoo, *J. Am. Chem. Soc.*, 2010, **132**, 2561.
 - G. DeBoer, J. W. Burnett and M. A. Young, *Chem. Phys. Lett.*, 1996, **259**, 368.
 - (a) T. Hertzsch, F. Budde, E. Weber and J. Hülliger, *Angew. Chem. Int. Ed.*, 2002, **41**, 2281; (b) L. Mohanambe and S. Vasudevan, *Inorg. Chem.*, 2004, **43**, 6421; (c) C. H. Görbitz, M. Nilsen, K. Szeto and L. W. Tangen, *Chem. Commun.*, 2005, 4288.
 - (a) J. Y. Lu and A. M. Babb, *Chem. Commun.*, 2003, 1346; (b) B. F. Abrahams, M. Moylan, S. D. Orchard and R. Robson, *Angew. Chem. Int. Ed.*, 2003, **42**, 1848; (c) L. Hashemia and A. Morsali, *CrystEngComm*, 2012, **14**, 779.
 - (a) H. J. Choi and M. P. Suh, *J. Am. Chem. Soc.*, 2004, **126**, 15844; (b) Z.-M. Wang, Y.-J. Zhang, T. Liu, M. Kurmoo and S. Gao, *Adv. Funct. Mater.*, 2007, **17**, 1523.
 - (a) G. M. J. Schmidt, *Pure Appl. Chem.*, 1971, **27**, 647; (b) G. Wegner, *Pure Appl. Chem.*, 1977, **49**, 443.
 - M. Nagarathinam, A. M. P. Peedikakkal and J. J. Vittal, *Chem. Commun.*, 2008, 5277.
 - (a) M. H. Mir, L. L. Koh, G. K. Tan and J. J. Vittal, *Angew. Chem. Int. Ed.*, 2010, **49**, 390; (b) D. Liu, Z.-G. Ren, H.-X. Li, J.-P. Lang, N.-Y. Li and B. F. Abrahams, *Angew. Chem. Int. Ed.*, 2010, **49**, 4767.
 - X.-Y. Wang, Z.-M. Wang and S. Gao, *Chem. Commun.*, 2007, 1127.
 - (a) M. H. Mir, S. Kitagawa and J. J. Vittal, *Inorg. Chem.*, 2008, **47**, 7728; (b) L. P. Zhang, W. J. Lu and T. C. W. Mak, *Polyhedron*, 2004, **23**, 169.
 - (a) M. Nagarathinam, J. J. Vittal and Macromol, *Rapid Commun.*, 2006, **27**, 1091; (b) A. M. P. Peedikakkal, L. L. Koh and J. J. Vittal, *Chem. Commun.* 2008, 441.